2020

Maximizing Bass Reflex System Performance Through Optimization of Port Geometry

Bryce Doll
University of Central Florida

MAXIMIZING BASS REFLEX SYSTEM PERFORMANCE THROUGH OPTIMIZATION OF PORT GEOMETRY

by

BRYCE DOLL

A thesis submitted in partial fulfillment of the requirements
for the Honors in the Major Program in Mechanical Engineering
in the College of Engineering and Computer Science
and in the Burnett Honors College
at the University of Central Florida
Orlando, Florida

Fall Term
2020

Thesis Chair: Hansen Mansy

Abstract

A bass-reflex system is a type of loudspeaker design that uses a port or a vent to improve low-frequency performance. The port acts as a Helmholtz resonator which extends the bass response of the system. However, at high drive levels, the air inside the port can become turbulent and cause distortion, noise, and compression. From previous works, it is known that the geometry of the port plays a crucial role in reducing these unwanted effects. This paper serves to provide more insight into optimal port shape by performing several objective tests on a group of 5 different prototype port shapes based on findings from previous literature. Total Harmonic Distortion (THD) and port compression tests were conducted to determine which port presented the highest performance.

Table of Contents

List of Figures

List of Tables

List of Acronyms

THD – Total Harmonic Distortion

NFR – Normalized Flare Rate

CFD – Computational Fluid Dynamics

FEA – Finite Element Analysis

MDF – Medium Density Fiberboard

1. Introduction

One current trend in loudspeaker design is to make speaker systems smaller in size while maintaining high performance. One way to increase the low-frequency performance of a loudspeaker system with size constraints is to add a port or a vent to the enclosure. This type of loudspeaker is known as a bass-reflex system and is the focus of this discussion.

First off, a loudspeaker is an apparatus that converts an electrical signal into sound. There are many different types of loudspeakers each with their own advantages and drawbacks. This paper will specifically discuss bass-reflex systems. This is a type of loudspeaker that uses a port or vent, cut into the speaker enclosure, to increase the efficiency of the system by introducing a Helmholtz resonator. Ported loudspeakers augment the bass response of the driver and can extend the frequency range of the system to lower frequencies compared to a sealed enclosure. However, some downsides come with these advantages. At high drive levels, air inside the port can become increasingly turbulent and cause distortion, noise, and compression. One main cause of these unwanted effects is vortex shedding. Vortex shedding occurs when an adverse pressure gradient develops, and the flow separates from the boundary i.e the port wall. This causes a flow reversal that induces a swirl like motion of the fluid. These swirl like currents or vortices have been determined to be the root cause of unwanted port noise otherwise known as “chuffing” [1]. This drawback will be the focus of this project.

Within a loudspeaker port, air particles undergo an oscillating internal flow dictated by the driver movement. If the boundary layer loses enough momentum during deceleration, the airflow can separate and reverse as it exits or enters the port. The most straightforward way to

reduce unwanted port noise is to reduce the flow velocity within the port by increasing the port's cross-sectional area. Increasing port area, however, also requires an increase in port length to maintain the same tuning frequency. This may not be feasible for designs with size limitations [2].

One main method engineers have used to reduce chuffing without increasing port cross-sectional area is by outwardly flaring the ends of ports. This method allows for higher flow velocities before separation and forces air exiting the port to slow down and dissipate into the surroundings in a more gradual and controlled manner. Gradual and even dispersion of the air's energy causes vortex shedding to be less extreme. As a result, flared ports can achieve output levels of 10 to 16 dB higher than that of straight ports before major distortion ensues [3]. This project will investigate 5 different flare rates. Specifically, the length of the straight section of the port will be altered with one port profile having a continuous curve with no straight section at all.

The purpose of this research is to add new insights into optimal port geometry by performing objective testing on several different port flare rates. Ultimately, this research will help aid the design optimization of loudspeaker ports and will allow for higher performing and better sounding bass-reflex systems.

2. Literature Review

Backman (1995) tested numerous port designs and compared their performance using total harmonic distortion (THD) and port compression measurements. THD is defined as the ratio between the energy within all harmonic frequencies of the output to the energy within the fundamental frequency of the input. THD measurements expose the total percentage of acoustic inaccuracies within the output of the speaker. Port compression is the measure of distortion present within the Helmholtz resonator i.e. the port. Port compression occurs at high drive levels where there is too much air trying to move through the port. At very high drive levels, airflow through the port stops almost completely, making the port no longer effective at all. Backman concluded that asymmetrical ports with sharp ends performed poorly and that more streamlined symmetric designs with rounded edges decreased turbulence and thus performed better. Backman also tested ports with constrictions and sharp bends and concluded that these structures are poor choices that can reduce the onset of turbulence by 3-5 dB and cause increased THD [2].

Vanderkooy (1997 & 1998) in 1997 goes on to test several different port designs with different lengths and profiles specifically focusing on port designs with flares and tapers. His paper presents the calculations needed to tune straight cylindrical ports and he then expands to propose a closed-form solution for the Helmholtz frequency of hyperbolic and cosine-hyperbolic port geometries. In conclusion, Vanderkooy stated that an optimal port shape should have all rounded edges, and the curved contour of the shape should be as gentle as possible [5].

In 1998 Vanderkooy expands this research by presenting the theory and measurements of a radial port velocity profile. He asserted that radial velocity profiles cannot be assumed to be uniform and that port flow velocities actually increase radially at low to moderate drive levels with instabilities beginning to occur within a port velocity range of 5 to 10 m/s [6].

Roozen (1998) proposed that unwanted port noise was the result of two different mechanisms. The first being the unsteady separation of the acoustic flow at the port end, and the second being boundary layer turbulence. Although the numerical solutions suggest that, at low drive levels, ports with small curvature radii produce less intense vortex shedding and therefore less port noise, it was seen after testing that ports with large curvature radii produced less intense vortex shedding. Roozen stated the most probable reason for this phenomenon is that ports with large curvature radii radiate noise less efficiently. At high velocities, the production of port noise is not only dependent on vortex intensity and noise radiation efficiency but is also dependent on the quality factor of the port. Quality factor is a dimensionless parameter that describes how dampened a resonator is. Resonators with high quality factors have low dampening so they ring or vibrate longer. For ports with small curvature radii, the quality factor significantly drops at high drive levels due to the transfer of energy from the acoustic oscillation to the free jet formed during vortex shedding. This type of interaction, however, is not as prominent for ports with large curvature radii. This led Roozen to conclude that higher quality factors for ports with large curvature radii compensate for the reduction of noise radiation efficiency at high amplitudes. Below in figures 1 and 2, the results from Roozen's numerical simulation are shown for two different port profiles. It can easily be seen in Figure 1 that flow separation occurs prematurely for ports that have higher curvature radii which reduces performance significantly.

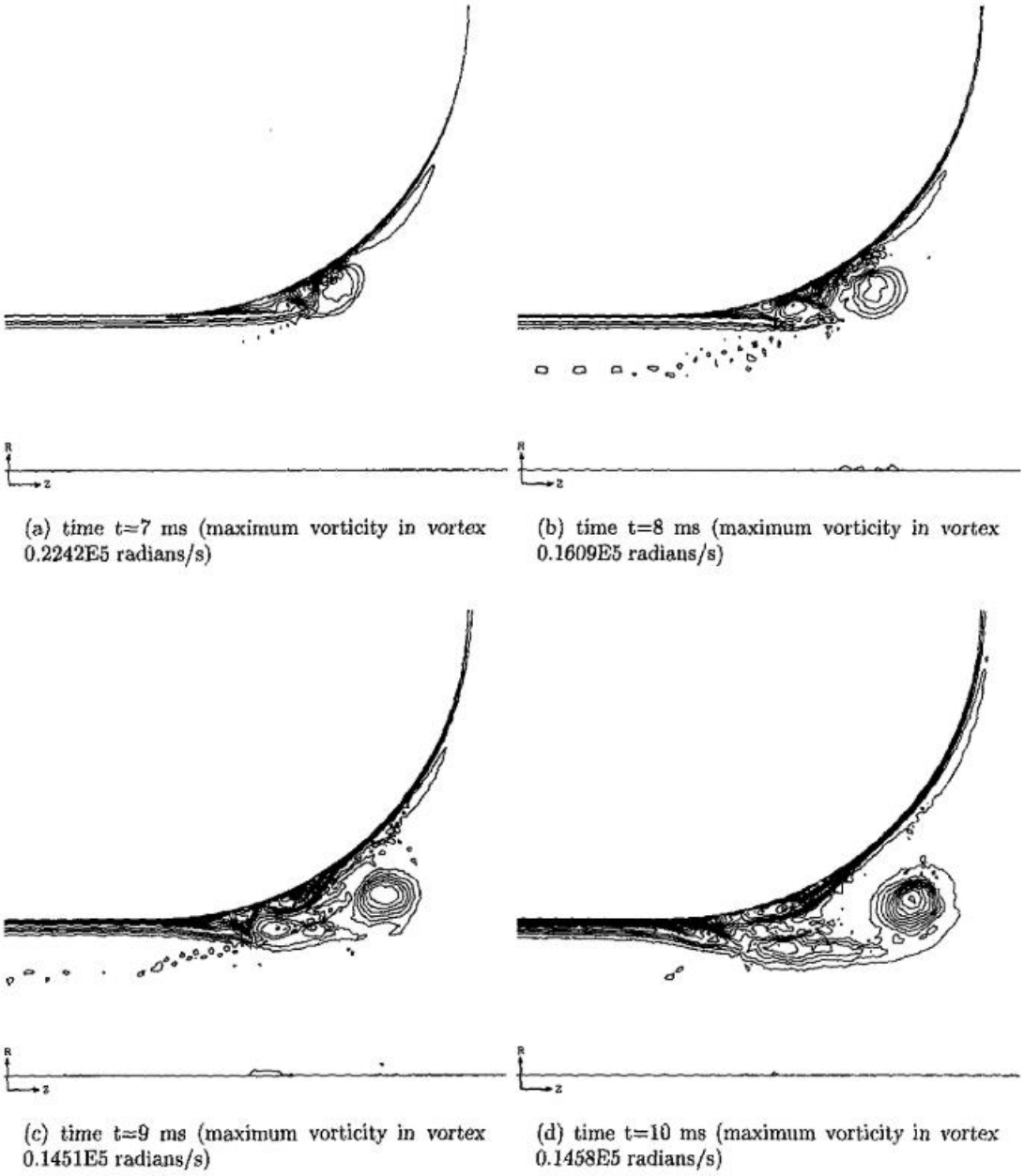

(a) time t=7 ms (maximum vorticity in vortex 0.2242E5 radians/s)

(b) time t=8 ms (maximum vorticity in vortex 0.1609E5 radians/s)

(c) time t=9 ms (maximum vorticity in vortex 0.1451E5 radians/s)

(d) time t=10 ms (maximum vorticity in vortex 0.1458E5 radians/s)

Figure 1 Simulation of vortex shedding in large curvature radii port on exit stroke. Note how early in the throat shedding begins.

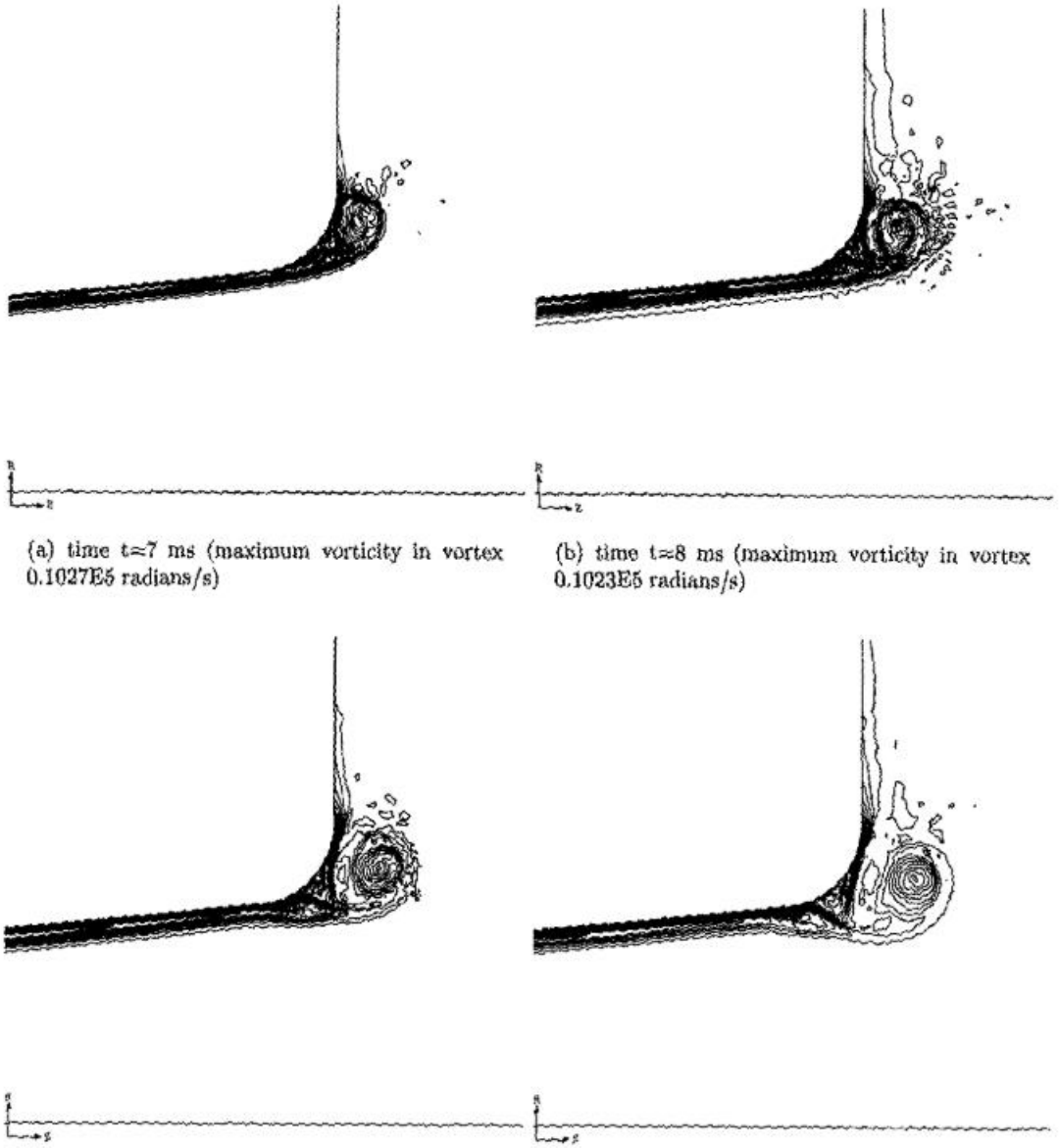

(a) time t≈7 ms (maximum vorticity in vortex 0.1027E5 radians/s)

(b) time t≈8 ms (maximum vorticity in vortex 0.1023E5 radians/s)

(c) time t≈9 ms (maximum vorticity in vortex 0.8776E4 radians/s)

(d) time t≈10 ms (maximum vorticity in vortex 0.839E4 radians/s)

Figure 2 Simulation of vortex shedding in small curvature radius port

Roozen also investigated port designs with converging-diverging tapers. From his numerical simulation, ports that are too generously tapered, taper angle above 6 degrees, can cause flow separation to occur before the port termination which significantly increases port noise. Roozen determined that a port that is slowly converging-diverging, so that separation does not occur prematurely, combined with a small radius end flare is optimal. Specifically, he stated that a port with a maximum converging-diverging taper angle of 6 degrees, measured between port contour and port axis, as compared to an identical straight port will produce 1 dB, 4 dB, and 5.5 dB less port noise for a sound power level of 85, 90, and 95 dB, respectively [7].

In 2002, Salvatti conducted several experiments and presented a normalized flare rate or NFR. NFR is described as the length of the port divided by two times the flare radius.

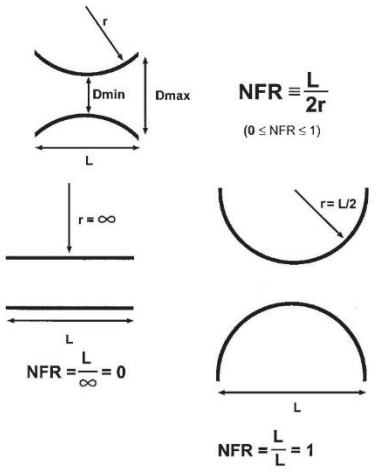

Figure 3 NFR Nomenclature

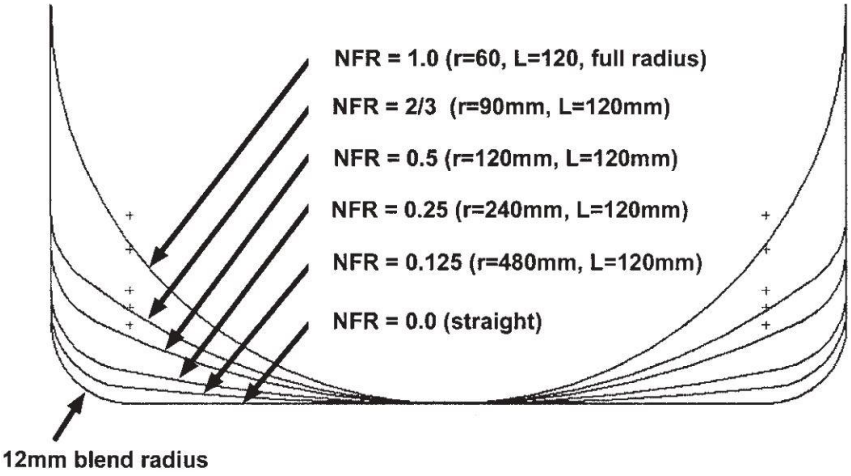

Figure 4 Illustration of NFR ranging from 0 to 1

First off, because a port with large curvature radii performs better at low drive levels but at high drive levels straighter ports perform better, Salvatti concluded that a moderately flared port with an NFR of 0.5 is the best compromise between the two. Also, Salvatti ran velocity profile measurements for a range of drive levels. From the results, straighter ports have the

highest velocities across an area that maps to the center hole diameter; beyond that and the velocity drops significantly. It can also be seen that moderately flared ports have a more evenly distributed velocity profile which leads to low port compression and higher achievable output. Figure 5 below shows the velocity measurements for 4 different port profiles.

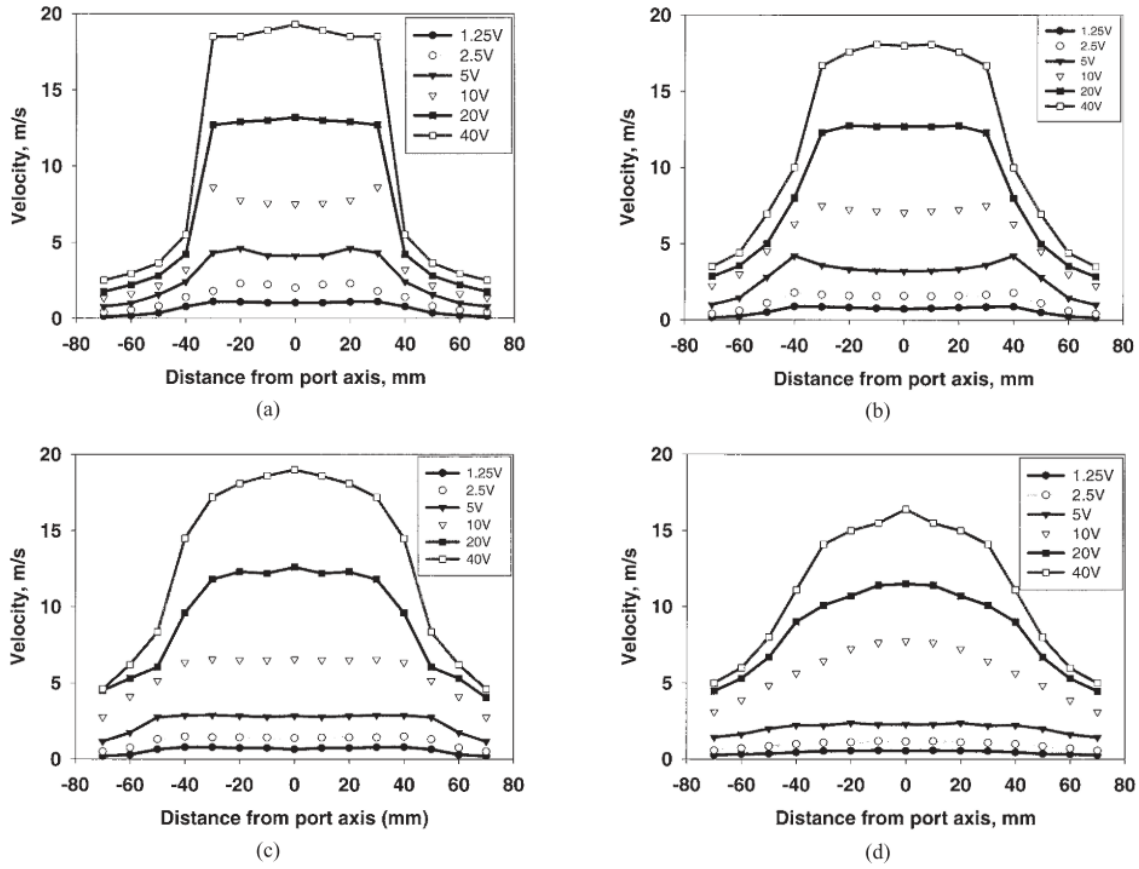

Figure 5 Port velocity profiles at 20 Hz. (a) No Flare. Note higher velocity at port edges for 10-V measurement. (b) Small Flare. 5-V measurement shows rise in velocity at edges. (c) Medium/Moderate Flare. Ports with NFR = 0.5 or higher do not show higher velocity at port edges. (d) Large Flare. [1]

One rather interesting issue that Salvatti investigated was the effect of surface roughness on port performance. Analogous to golf ball aerodynamics, roughening the surface of the port should reduce drag and delay flow separation thus resulting in less port noise. Using spray adhesive, Salvatti affixed small glass beads ranging in size from 1 to 2.5 mm to the inside of the

port. Once compared to an identical smooth port, it was seen that rough ports were generally inferior in terms of performance. The inferior performance is most likely the result of the complex oscillatory nature of the flow [1].

Devantier (2004) employed the use of CFD to model several different port profiles over different sound levels. The model and the empirical data suggested that at low drive levels, <10 dB, THD decreased with increasing drive level. This suggests the THD is below the noise floor of the measurement. At moderate drive levels, between 10- 20 dB, THD decreases as flare rate increases. However, at high drive levels, > 20 dB, the relatively moderately flared port had the lowest THD. This indicates that, for high drive levels, high flare rates are not always optimal. Overall Devantier concluded that if a port's flare is too gentle, flow separation will occur first at the inlet stroke. If a port has too much flare, flow separation will occur prematurely within the port upon exit. He stated that the optimal solution is one that delays the occurrence of both of these events to the highest possible level [8].

In 2019, Bezzola's work demonstrated that there is indeed an optimal flare rate for bass-reflex ports. His hypothesis is based on linear acoustic FEA simulation and observations of the particle velocity profile at port exit. These simulations are much more efficient than solving turbulent flow with numerically expensive CFD analysis. Bezzola proposed that a flat particle velocity contour at port exit is optimal for the reduction of unwanted port noise. This notion was confirmed through acoustic testing of 8 different port profiles. His tests suggested that port shapes with the flattest particle velocity profiles showed less port noise and also achieved higher drive levels before the onset of flow separation as shown from port compression measurements. Multiple blind listening tests were also conducted which demonstrated that ports with flat

particle velocity profiles were rated better at all drive levels with the most significant differences arising at drive levels above 95 dB. With this, Bezzola presented a simple iterative method to produce port shapes with flat velocity profiles at exit. Ultimately, Bezzola's method is a very efficient design flow that has been tested and validated. His method stands to be the most comprehensive and proven approach to optimal port design thus far [3]. However, more studies are needed to confirm these results.

Typically, when designing a port, the main limiting factor is the length which is dictated by the internal dimensions of the enclosure. Ports that are longer in length allow for a larger internal diameter which reduces the flow velocity within the port. As high flow velocities cause the onset of turbulence, the largest internal diameter that yields a port that satisfies the length restriction is optimal. Flaring a port allows for higher flow velocities before turbulence ensues and, from previous literature, it has been concluded that a port flare rate that has the least amount of entrance loss and lowest propensity for premature flow separation on the exit stroke will perform the best. To explain this further, Salvatii's normalized flare will be used for reference.

On the inlet stroke, the most consistent gradual curve is optimal as it provides the least entrance loss. A graph plotting resistance coefficient, K, as a function of blend radius is presented below.

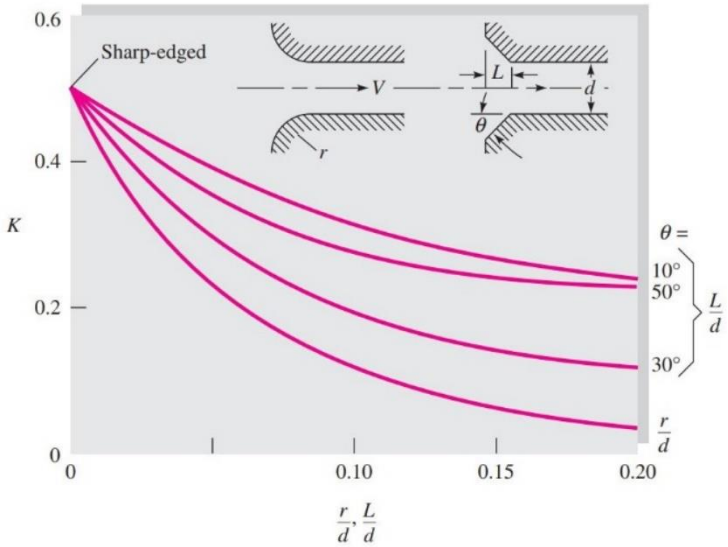

Figure 6 Entrance loss for a cylindrical pipe as a function of blend radius and entrance angle [9]

From the graph, it is apparent that the largest blend radius will provide the least entrance loss. This would equate to an NFR of 1. However, with this configuration, flow separation on the exit stroke will occur prematurely within the port at high drive levels. This phenomenon is best illustrated in figure 1 within the literature review. For the exit stroke, the highest flare radius achievable before flow separation begins to occur prematurely within the port is optimal. This flare rate depends on the flow velocity and thus the drive level. This means for extremely high drive levels an NFR of 0 performs best. With all of this in mind, the optimal flare rate for a bass-reflex system designed to operate at various drive levels would meet in the middle of these two extremes.

3. Methodology

3.1 Port Profile Selection

One of the main limitations to the port geometry selection was the capabilities of the 3d printer. Overhang angles below 40° did not print well and thus were avoided. Also, print time was another limiting issue considered. This limited the overall size of the ports as larger ports could take over a week to print.

Because ports with continuous flares have been thoroughly investigated, this study serves to analyze the effect of adding a straight section in the middle of the port. To execute this, a port aspect ratio (ratio of length to inner diameter) of 3:1 was selected as it allowed for adjustment of the straight section length while still providing flare radii that were not too sharp or too shallow. These flare radii were in the range of ports tested in previous literature. The calculations from WinISD (lumped parameter simulation software) determined a port length of 24.7cm with an inner diameter of 8.25cm for the given enclosure size. The overall length, inner diameter, and outer diameter of each port were maintained constant to ensure similar port tunning. The only geometric parameter changed between each port was the length of the straight section with the initial straight section length being 1/3 the total length (8.23cm). Each straight section length was then reduced by 33% until both end flares met in the middle forming one continuous curve. This led to 4 different port profiles with the fifth being a straight port as a benchmark with a simple blend radius of 0.25cm. Each of the 4 flared ports was given a 1.25cm blend radius to ensure there were no sharp discontinuities at the port end. The curve between the straight section and

the outer diameter was a simple tangent curve dictated by the straight section length. A table describing the geometric parameters as well as a schematic for each port is presented below.

Table 1 Port Dimensions

Port #	Straight Section Length (cm)	Curvature Radii (cm)	Blend Radius (cm)	Inner Diameter (cm)	Outer Diameter (cm)	Length (cm)	Aspect Ratio (Length to Inner Diameter)
1	8.23	10.58	1.25	8.25	17.10	24.70	3:1
2	5.48	13.70	1.25	8.25	17.10	24.70	3:1
3	2.74	17.28	1.25	8.25	17.10	24.70	3:1
4	0	21.34	1.25	8.25	17.10	24.70	3:1
5	N/A	N/A	0.25	8.25	17.10	24.70	3:1

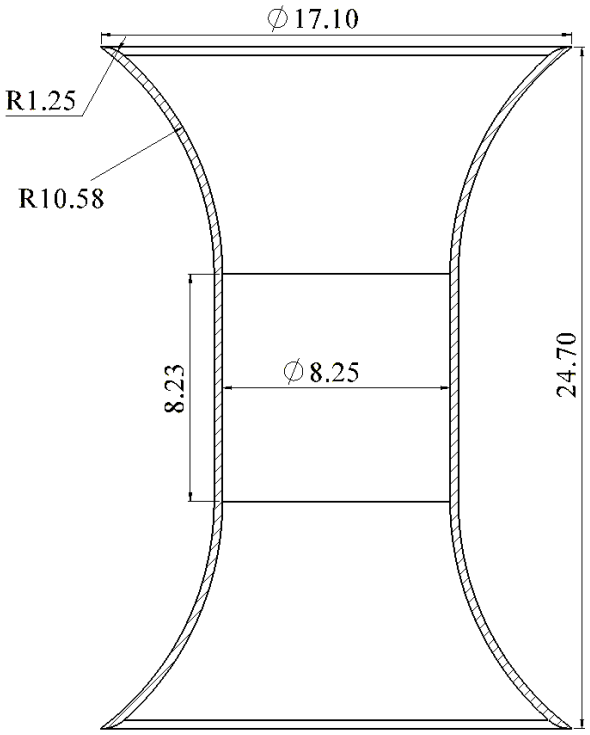

Figure 8 Port 1 Schematic

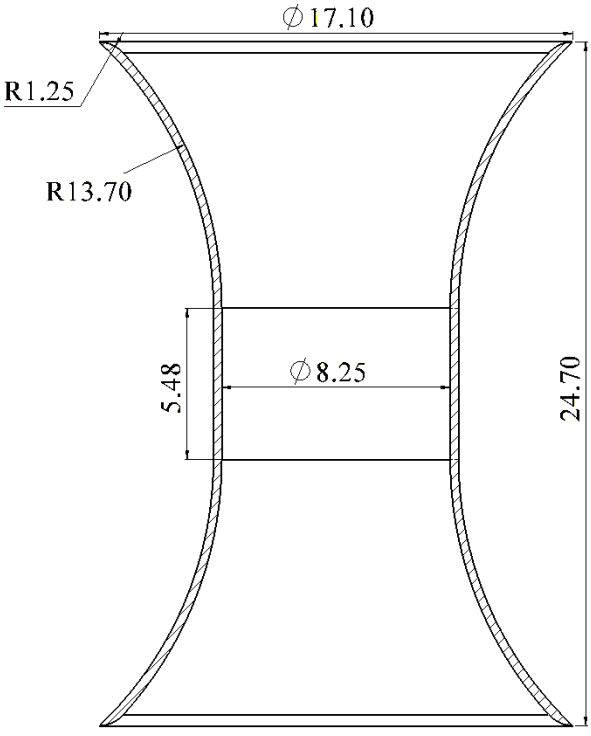

Figure 7 Port 2 Schematic

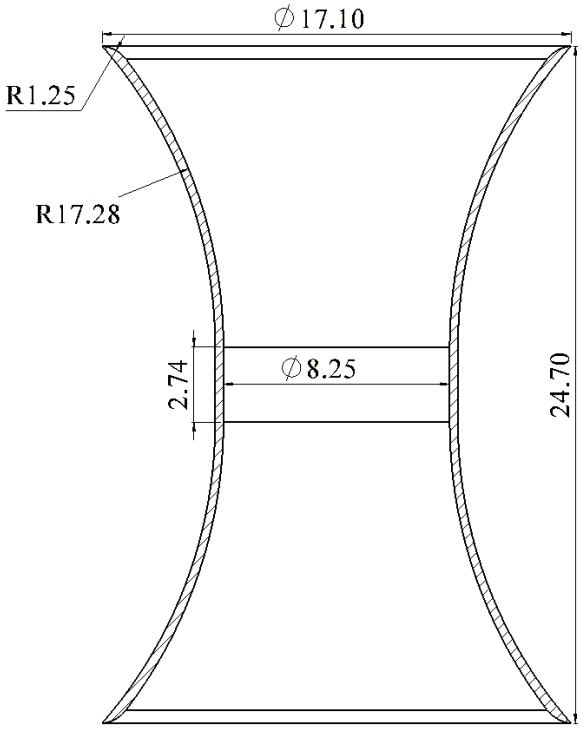

Figure 9 Port 3 Schematic

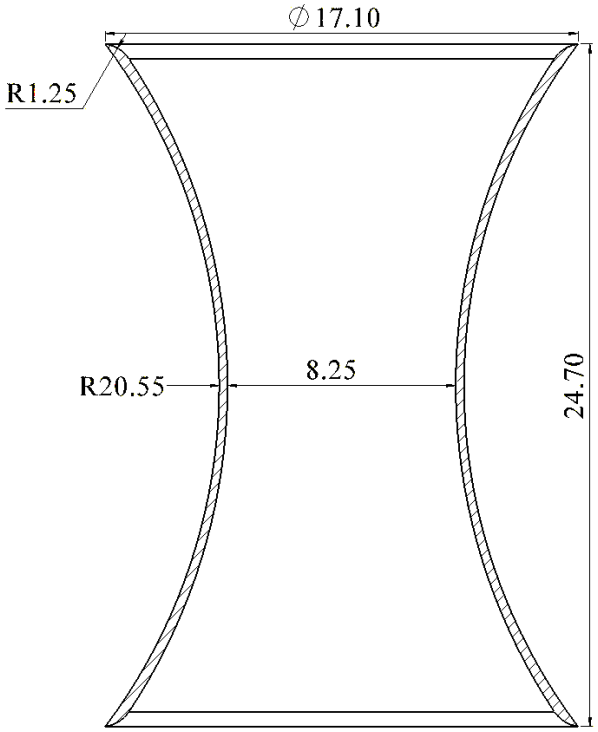

Figure 10 Port 4 Schematic

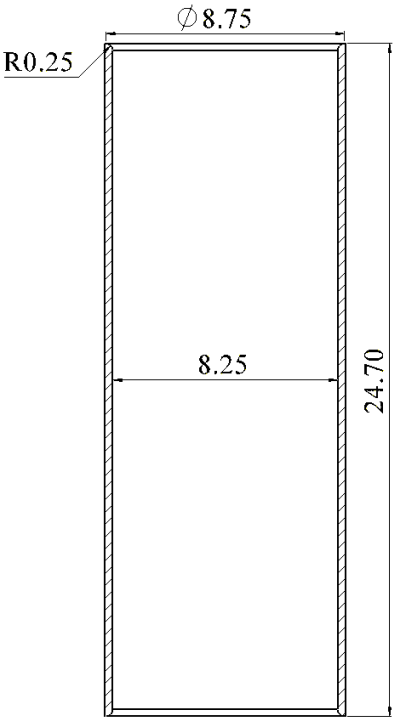

Figure 11 Port 5 Schematic

3.2 Experimental Setup

To determine port performance, each port was subject to THD and port compression measurements. These measurements were conducted using a single high excursion 10-inch subwoofer driver mounted to a 3.70ft^3 MDF (medium density fiberboard) enclosure. The enclosure walls were 3/4in thick and the mounting surface was double baffled for extra stability. The subwoofer was powered by a Dayton Audio SA100 100-watt plate amplifier, and the voltage measurements were recorded using an Owon VDS1022I PC oscilloscope. All acoustic measurements were performed by the Dayton Audio Omnimic v2 microphone, and the data acquisition was run through a PC using the Omnimic and Owon software provided by each of the units.

Each port was externally mounted on the backside of the enclosure opposite the driver. This was to provide an easy method to change between ports as well as keep the port output isolated from the driver output. An external baffle was also implemented for symmetry as well as to provide more sound isolation from the driver. A list of equipment, as well as a schematic of the test setup, is presented below.

List of equipment:

- Subwoofer: Dayton Audio W10424A
- Amplifier: Dayton Audio SA100
- Oscilloscope: Owon VDS1022I
- Microphone: Omnimic v2

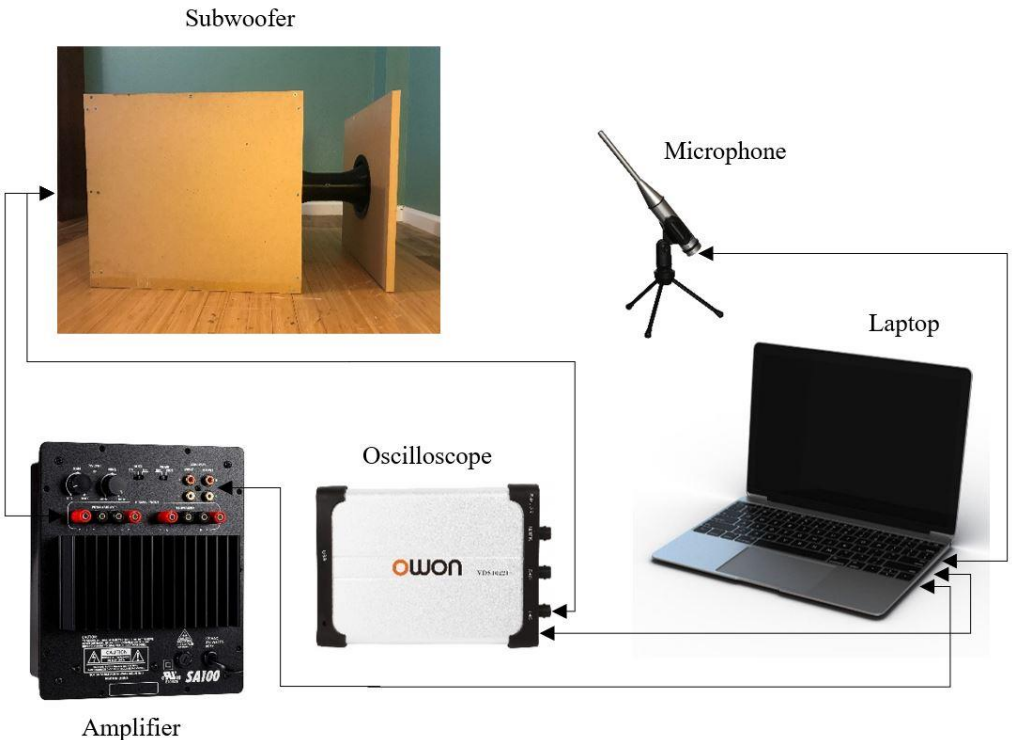

Figure 12 Test Setup Schematic

3.3 Test Procedure

To begin, the port understudy was first subject to a harmonic distortion test. This entailed positioning the Omnimic on axis just 15cm away from the port. As room reflections are very detrimental to the measurement of harmonic distortion, a closer measurement position allowed for sound coming from the port to be much stronger than those coming from reflections. The placement of the Omnimic and the enclosure were then marked off to ensure that microphone positioning and room acoustic effects were equal for all subsequent tests. The room temperature was also considered and was kept constant at 72°F. This was to ensure any thermal effects remained constant between tests. With everything in position, a long sine sweep provided and generated by the Omnimic software was played. A total of 20 sweeps were played and averaged by the Omnimic software to form the final data set. Total harmonic distortion was calculated

using Farina's method [10]. This method involves an exponentially swept sine signal as stimulus. Then the result is deconvolved to an impulse response where distortion appears in negative time relative to the time instant of the main impulse response. The various products (2nd through 5th order harmonic distortion) are obtained by taking a Fourier transform of the distortion impulse responses.

Next, the port understudy was subject to a port compression test. Port compression is defined as the nonlinearity presented in the transfer function between the sound pressure output and the input power. The test entailed placing the Omnimic on axis 1 meter away from the port. Again, the exact position of the Omnimic was marked for future tests. The port compression test was conducted by incrementally increasing the drive level of a 30Hz sine signal from 0.05Vrms to the maximum amplifier output of 2.433Vrms. After each increment, the dBSPL was recorded measured by the Omnimic. A 30Hz signal was chosen because it produced the most output within the augmented response range of the system.

4. Experimental Results

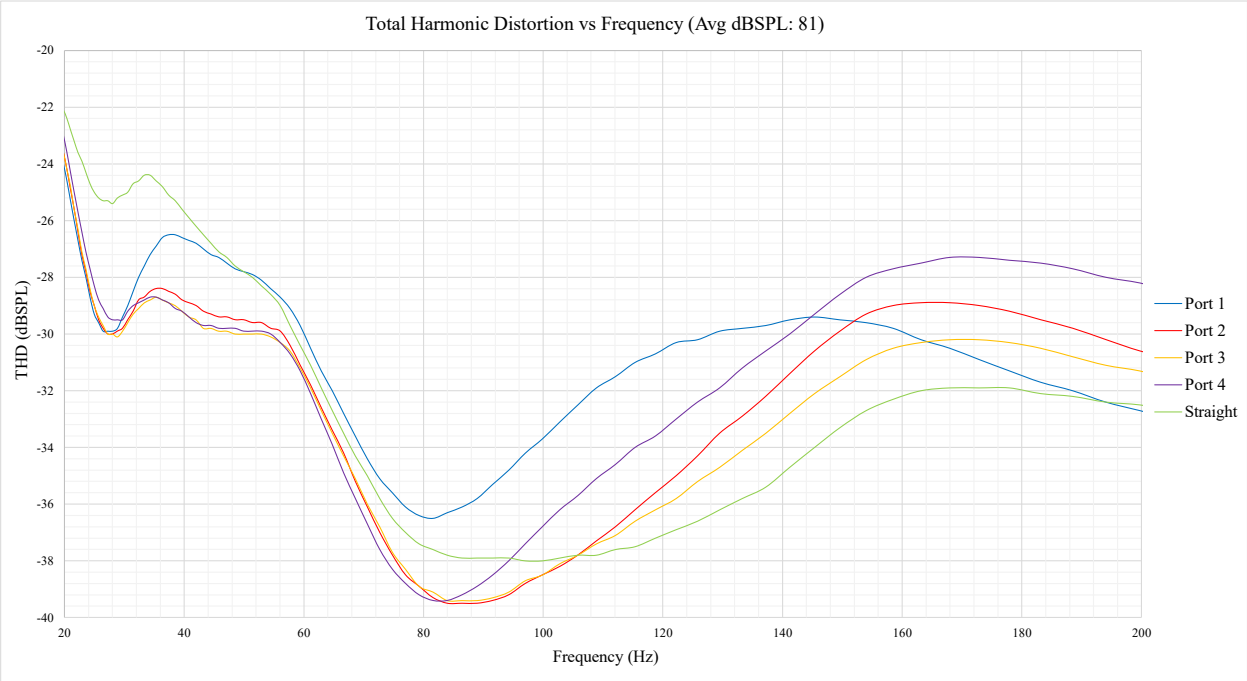

Figure 13 THD vs Frequency (Low Drive Level)

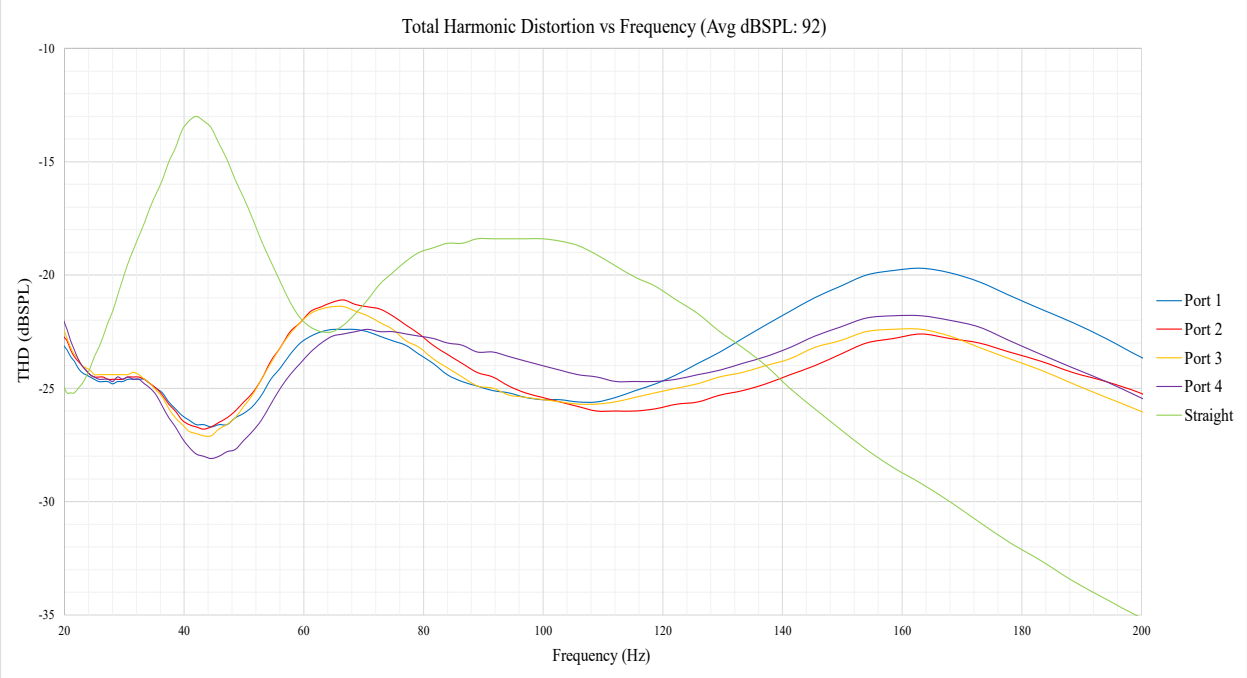

Figure 14 THD vs Frequency (Medium Drive Level)

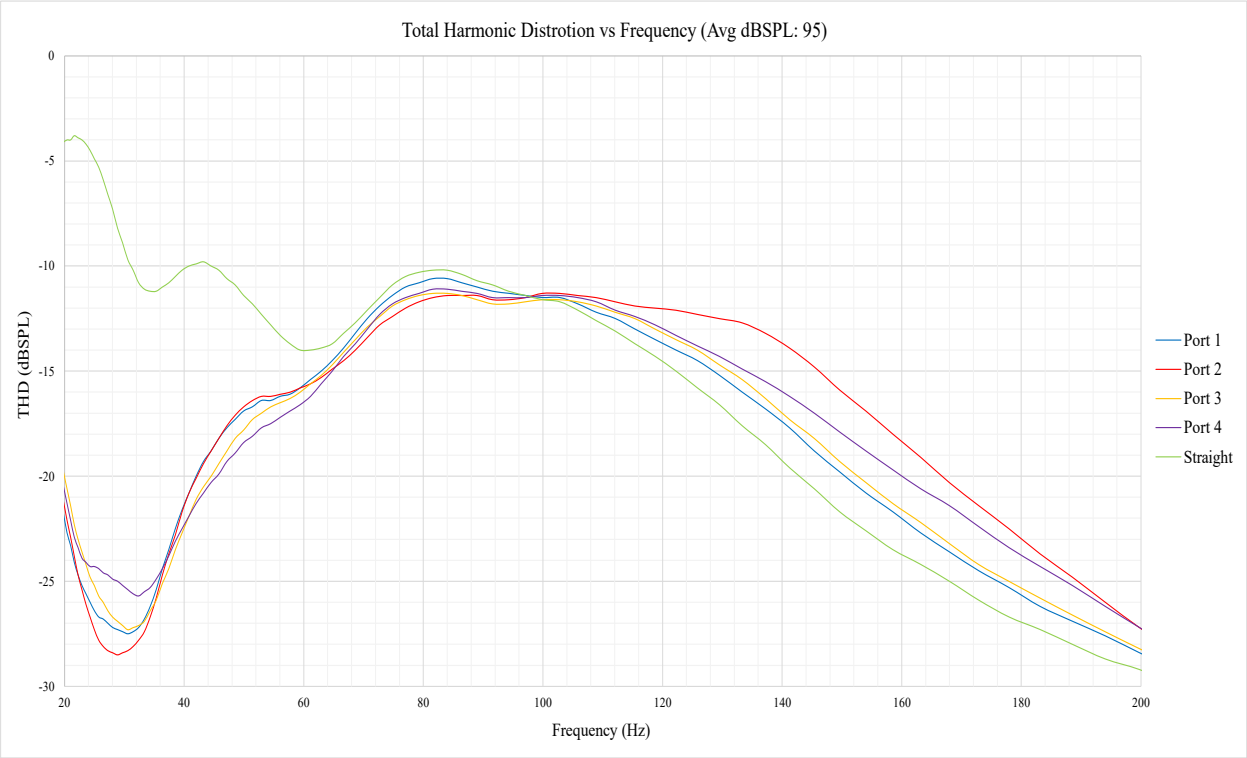

Figure 15 THD vs Frequency (High Drive Level)

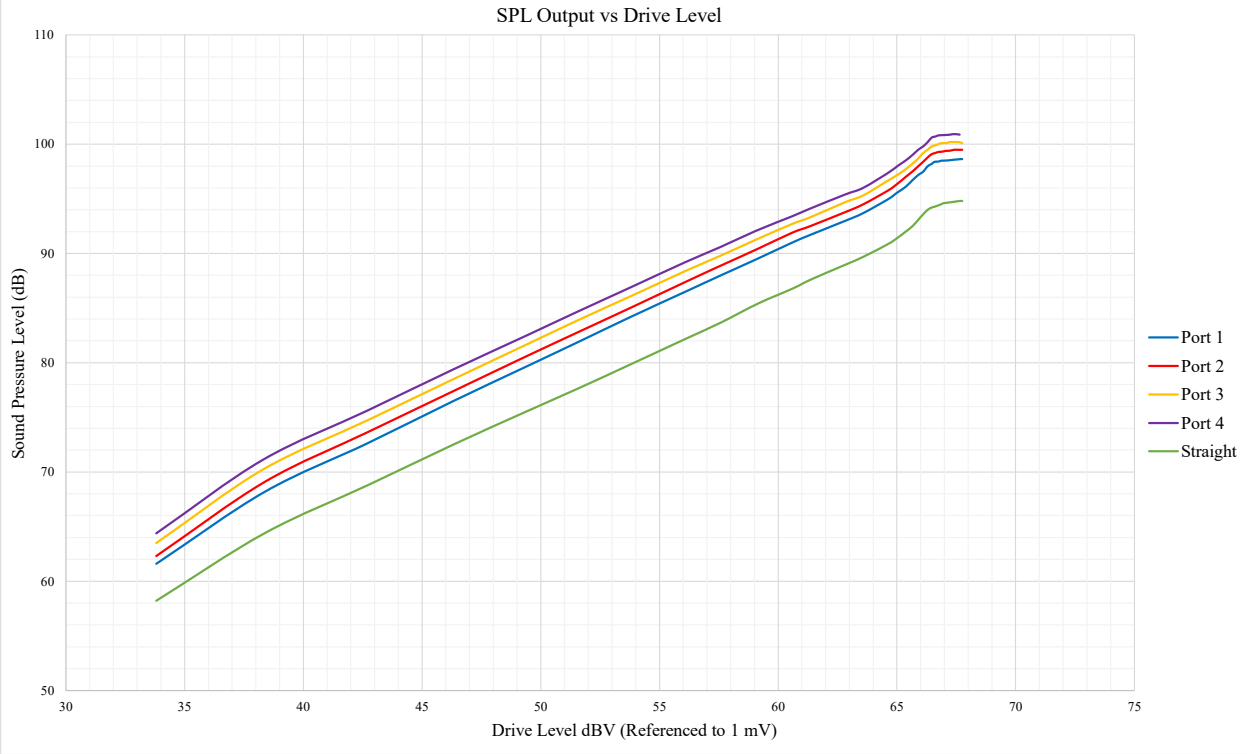

Figure 16 SPL Output vs Drive Level

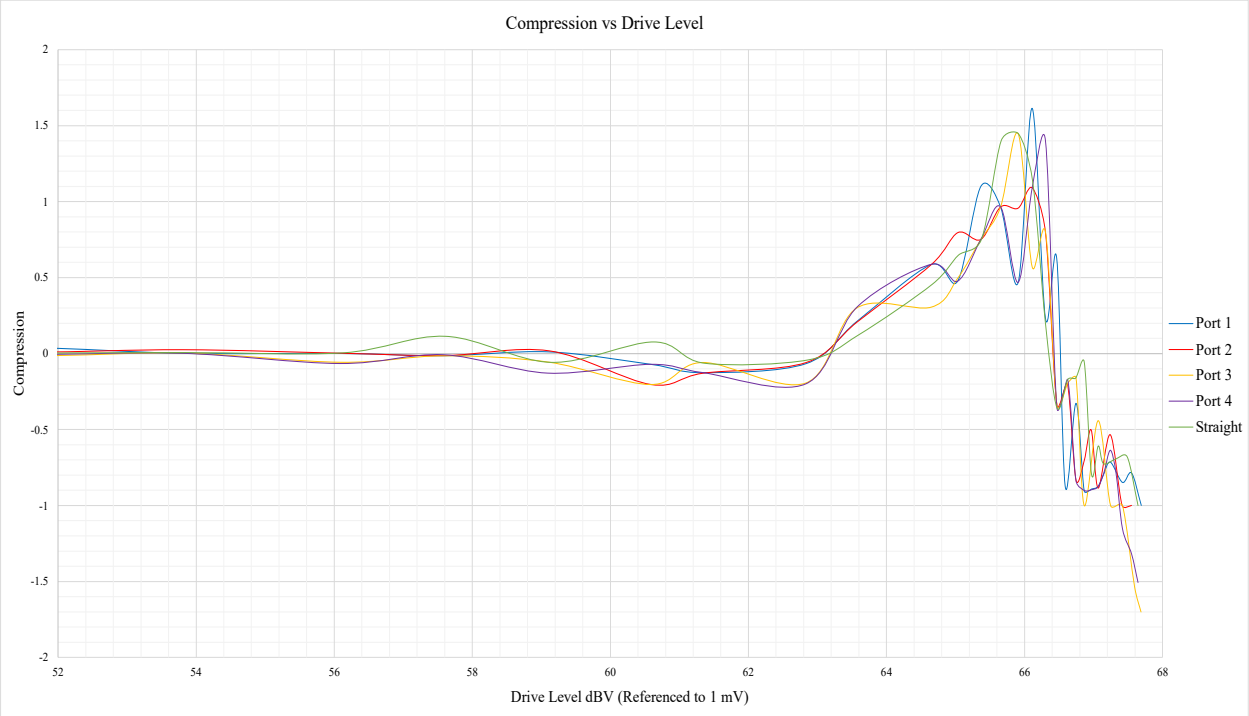

Figure 17 Port Compression vs Drive Level

5. Discussion

5.1 Measurement Limitations

Due to limiting circumstances, the experiments performed in this study were conducted in a small room with abnormal geometry. As harmonic Distortion measurements are especially susceptible to room reflections, these tests ideally should have been conducted in an anechoic chamber. However, the precision of the results was validated by performing each test multiple times and observing the variation in the results. The variation was small and averaging was used to provide a more precise representation. A second set of validation testing was performed by slightly altering the microphone position between tests and comparing the results. A strong dependence on microphone positioning was found. This again is due to room acoustics. With this in mind, the distortion measured is both a product of the port and also the room. This means only comparison between ports can be made assuming room acoustic effects remain constant between tests.

5.2 Harmonic Distortion

The first of the harmonic distortion measurements were conducted at low drive level with an average fundamental output of 53dBSPL. It is noted that port 1 and the straight port generally had higher distortion than the rest of the group at the lower end of the frequency range. At low drive levels, more generously flared ports will have less distortion. This is because low drive levels present lower flow velocities within the port and thus more generous flare rates can be implemented without premature flow separation on the exit stroke.

The second harmonic distortion graph is characterized by medium drive level with an average fundamental output of 92dBSPL. At this drive level, performance between ports is remarkably similar excluding the straight port. The sporadic nature of the straight port's distortion is unknown but can mostly be attributed to measurement error.

The last of the harmonic distortion graphs presents the distortion at a high drive level with an average fundamental output of 95dbSPL. Significant differences occur near the system tunning frequency where port 2 had the lowest distortion and port 4 had the highest. At extremely high drive levels, the straight port would be expected to have the lowest distortion. However, the capabilities of the amplifier did not merit extremely high drive levels and an average of 95dBSPL was at the limit. If higher drive levels were implemented, a different test approach would be needed as Farina's method plays a long sine sweep from 5 to 10K hertz. Playing such low frequencies at high power would present high distortion within the subwoofer and may also cause damage to the driver by over-excursion.

5.2 Port Compression

From the results of the compression measurements, it can be seen that nonlinearities begin around 54 dBSPL. From this point, there are three distinct regions to note. The first being the region ranging from 54 to 64 dBSPL. This region is the start of the transition from laminar to turbulent flow and is where compression is first observed. From 64 to 66 dBSPL a compression reversal occurs. This has been observed by multiple other studies and was first noted by Salvatti [1]. It has been postulated that this point marks the onset of turbulence where port losses are actually reduced. This reversal period extends to just beyond 66 dBSPL. From there, the last region is characterized by a sharp reversal where compression is accelerated. This is where full flow separation begins, and vortex shedding occurs.

It can also be noted from the SPL output graph that port 4, the most generously flared port, achieved the highest output and that port 5, the straight port, had the lowest output. This was expected as the more generously flared ports had a larger average internal diameter. This allows them to reach higher flow velocities before reaching the critical Reynolds number where laminar to turbulent flow transition begins. This transition is the cause of the onset of compression. Also, a larger average internal diameter

provides a larger port air volume. This, in turn, allows more air to move creating higher sound pressure levels.

6. Conclusion, Limitations, & Future Work

6.1 Conclusion

All in all, the harmonic distortion tests presented high dependence on frequency. However, this may be a product of acoustic reflections from the room. More testing is needed to verify this. In terms of output, port 4 had the highest which was expected as it has the largest internal volume and can move the most air. For the compression measurements, all ports including the straight port started to compress around the same drive level. From previous studies, straight ports started to compress at significantly lower drive levels than that of flared ports. It is unknown why this occurred. To improve the accuracy of the results, testing in an anechoic chamber would be ideal but access to such facilities is limited. Outdoor testing may be a possible solution as large spaces minimize reflections. Also, a microphone that allows for direct observation of the voltage measurements would be ideal as the Omnimic is limited to only perform the calculations within its compatible software.

6.2 Limitations

There were many limitations encountered when performing this study. One of them being access to university facilities. Due to unfortunate circumstances, access to such facilities was not possible. With this, all test equipment included the 3d-printer had to be acquired remotely. Also, the testing which was planned to take place at the university had to be conducted remotely. Many larger indoor spaces at the university would have reduced measurement inaccuracies due to room acoustics. This presented many challenges that were not in the original scope of the project. For example, a much more capable 3-D printer was available at the university. Not having access to this not only limited the possible dimensions and quality of the prototype ports but also much time was lost researching and acquiring all the equipment

necessary to prototype and test each port. Money was also a limiting factor on what equipment could be acquired. Another major limitation was proximity to the thesis committee as well as other colleagues. Due to the circumstances, remote communication was required which hindered progress.

The Omnimic also presented some limitations on the type of calculations that could be performed from the raw voltage measurements. With the Omnimic, Farina's method is the only way THD could be calculated. Farina's method measures THD over a large frequency range of 5 to 10k Hz. However, such a wide range is not necessary because the typical operating range of a subwoofer is only 20 – 100 Hz. Ideally, given that optimum port shape is dependent on drive level, a THD test that focused on one frequency at a time with incrementally increasing drive level would be optimal.

6.3 Future Work

Moving forward, the main priority is to first conduct more research on loudspeaker simulation and testing methods. FEA simulation using Ansys Fluent and COMSOL's acoustics module will be implemented to predict port performance and objective testing will be performed to validate these models. Once validated, the models will be used to choose new port profiles to test. Also, a new measurement microphone that allows direct manipulation of the voltage measurements will be acquired for future testing, and new test environments will be explored as well to limit the effects of room acoustics on the results.

References

[1] Salvatti, A., Devantier, A., & Button, D. J. (2002). Maximizing Performance from Loudspeaker Ports. *Audio Engineering Society, 50*(1/2), 19–45-19–45. Retrieved from http://www.aes.org/e-lib/browse.cfm?elib=11094

[2] Backman, J. (1995). The Nonlinear Behavior of Reflex Ports. *Audio Engineering Society*. Retrieved from http://www.aes.org/e-lib/browse.cfm?elib=7767

[3] Bezzola, A., Devantier, A., & McMullin, E. (2019). Loudspeaker Port Design for Optimal Performance and Listening Experience. *Audio Engineering Society*. Retrieved from http://www.aes.org/e-lib/browse.cfm?elib=20683

[4] Lin, J. C. (2002). Review of research on low-profile vortex generators to control boundary-layer separation. *Progress in Aerospace Sciences, 38*(4), 389-420. doi:https://doi.org/10.1016/S0376-0421(02)00010-6

[5] Vanderkooy, J. (1997). Loudspeaker Ports. *Audio Engineering Society*. Retrieved from http://www.aes.org/e-lib/browse.cfm?elib=7256

[6] Vanderkooy, J. (1998). Nonlinearities in Loudspeaker Ports. *Audio Engineering Society*. Retrieved from http://www.aes.org/e-lib/browse.cfm?elib=8432

[7] Roozen, N. B., Vael, J. E. M., & Nieuwendijk, J. A. (1998). Reduction of Bass-Reflex Port Nonlinearities by Optimizing the Port Geometry. *Audio Engineering Society*. Retrieved from http://www.aes.org/e-lib/browse.cfm?elib=8519

[8] Devantier, A., & Rapoport, Z. (2004). Analysis and Modeling of the Bi-Directional Fluid Flow in Loudspeaker Ports. *Audio Engineering Society*. Retrieved from http://www.aes.org/e-lib/browse.cfm?elib=12851

[9] White, F. M., & Chul, R. Y. (2016). *Fluid mechanics*. New York: McGraw-Hill education.

[10] Farina, A. (2000). Simultaneous Measurement of Impulse Response and Distortion With a SweptSine Technique. *Audio Engineering Society*. Retrieved from https://www.aes.org/e-lib/browse.cfm?elib=10211